NeuroImage: Clinical 29 (2021) 102562

Contents lists available at ScienceDirect

NeuroImage: Clinical

journal homepage: www.elsevier.com/locate/ynicl

# Lesion distribution and substrate of white matter damage in myotonic dystrophy type 1: Comparison with multiple sclerosis

Sara Leddy [a,b], Laura Serra [c], Davide Esposito [a], Camilla Vizzotto [a], Giovanni Giulietti [c], Gabriella Silvestri [d], Antonio Petrucci [e], Giovanni Meola [f,g], Leonardo Lopiano [h], Mara Cercignani [a,c], Marco Bozzali [a,e,*]

[a] Clinical Imaging Sciences Centre, Brighton and Sussex Medical School, Brighton, United Kingdom
[b] Brighton and Sussex University Hospital Trust, Brighton, United Kingdom
[c] Neuroimaging Laboratory, Santa Lucia Foundation, Rome, Italy
[d] Department of Neuroscience, Fondazione Policlinico Gemelli IRCCS, Università Cattolica del S. Cuore, Rome, Italy
[e] UOC Neurologia e Neurofisiopatologia, AO San Camillo Forlanini, Rome, Italy
[f] Department of Neurorehabilitation Sciences, Casa di Cura Policlinico, Milan, Italy
[g] Department of Biomedical Science for Health, University of Milan, Milan, Italy
[h] 'Rita Levi Montalcini' Department of Neuroscience, University of Torino, Turin, Italy

ARTICLE INFO

*Keywords:*
DM1
qMT
MS
Lesion
White matter
MRI

ABSTRACT

Myotonic Dystrophy type 1 (DM1) is an autosomal dominant condition caused by expansion of the CTG triplet repeats within the myotonic dystrophy protein of the kinase (DMPK) gene. The central nervous system is involved in the disease, with multiple symptoms including cognitive impairment. A typical feature of DM1 is the presence of widespread white matter (WM) lesions, whose total volume is associated with CTG triplet expansion. The aim of this study was to characterize the distribution and pathological substrate of these lesions as well as the normal appearing WM (NAWM) using quantitative magnetization transfer (qMT) MRI, and comparing data from DM1 patients with those from patients with multiple sclerosis (MS). Twenty-eight patients with DM1, 29 patients with relapsing-remitting MS, and 15 healthy controls had an MRI scan, including conventional and qMT imaging. The average pool size ratio (F), a proxy of myelination, was computed within lesions and NAWM for every participant. The lesion masks were warped into MNI space and lesion probability maps were obtained for each patient group. The lesion distribution, total lesion load and the tissue-specific mean F were compared between groups. The supratentorial distribution of lesions was similar in the 2 patient groups, although mean lesion volume was higher in MS than DM1. DM1 presented higher prevalence of anterior temporal lobe lesions, but none in the cerebellum and brainstem. Significantly reduced F values were found within DM1 lesions, suggesting a loss of myelin density. While F was reduced in the NAWM of MS patients, it did not differ between DM1 and controls. Our results provide further evidence for a need to compare histology and imaging using new MRI techniques in DM1 patients, in order to further our understanding of the underlying disease process contributing to WM disease.

## 1. Introduction

Myotonic dystrophy type 1 (DM1) is an autosomal dominant disorder caused by an expansion of the trinucleotide CTG repeat motif. Found on chromosome 19, the repeat motif is in the 3′UTR of the DMPK gene, located at point 13.3 (Brook et al., 1992; Fu et al., 1993; Mahadevan et al., 1993). DM1 affects at least 1 in 8000 people worldwide and is the most common form of neuromuscular disorder with clinical onset in adulthood (Emery, 1991; Meola & Cardani, 2015). DM1 is a multisystem disorder affecting the heart, both smooth and skeletal muscle, the eyes, endocrine system, central and peripheral nervous system (Romeo, 2012; Schara and Schoser, 2014; Turner & Hilton-Jones, 2014; Ashizawa et al., 2018). Post-mortem examinations of the brain of people with DM1 have highlighted the presence of nuclear RNA foci (i.e., CTG repeats) (Jiang et al., 2004), and of neurofibrillary tangles, leading to the disease being considered a tauopathy (Yoshimura et al., 1990; Vermersch et al., 1996).

* Corresponding author at: 'Rita Levi Montalcini' Department of Neuroscience, University of Torino, Via Cherasco, 15, 10126 Turin, Italy.
*E-mail address:* marco.bozzali@unito.it (M. Bozzali).

https://doi.org/10.1016/j.nicl.2021.102562
Received 7 September 2020; Received in revised form 6 January 2021; Accepted 8 January 2021
Available online 14 January 2021

Although adult onset DM1 patients typically present with preserved global cognition at formal testing (Di Costanzo et al., 2002; Minnerop et al., 2011; Serra et al., 2015), when examined more closely, detailed cognitive testing has revealed executive and memory dysfunctions (Meola et al., 2003; Modoni et al., 2004; Weber et al., 2010) as well as dysfunction of social cognition (Serra et al., 2016, 2020), and pathological personality traits (Serra et al., 2014), partially explained by altered functional connectivity (Serra et al., 2014, 2016) and reduced regional cortical thickness (Serra et al., 2020).

Imaging of the brains of those affected by DM1 demonstrates structural damage in both the grey and white matter, but predominantly white matter. Magnetic resonance imaging (MRI) studies described the presence of ventricular dilatation and periventricular hyperintensities (Glantz et al., 1988; Hund et al., 1997; Di Costanzo et al., 2002; Minnerop et al., 2011; Caso et al., 2014), resembling lesions detected in other conditions such as multiple sclerosis (MS) (Damian et al., 1994), Lyme disease (Fernandez et al., 1990), and coeliac disease (Kieslich et al., 2001). Other common findings include cerebral atrophy (Minnerop et al., 2011; Serra et al., 2015), and enlarged Virchow-Robinson spaces (Di Costanzo et al., 2001). Interestingly, the white matter lesion load, regional grey matter volumes, and white matter microstructure were all reported to correlate with patient CTG triplet expansion (Serra et al., 2015; Zanigni et al., 2016; van der Plas, et al., 2019). Using conventional MRI, white matter T2-hyperintense lesions in the anterotemporal and temporopolar regions have been repeatedly reported by studies as areas of typical change in DM1 patients (Huber et al., 1989; Miaux et al., 1997; Abe et al., 1998; Ogata et al., 1998; Di Costanzo et al., 2001; Zanigni et al., 2016). Anterior temporal lobe lesions differ to other lobar lesions seen in DM1, as they appear to involve the arcuate fibres, a feature not seen in lobar lesions. The MRI pattern of distribution, asymmetry of white matter lesions, involvement and sparing of specific structures is thought to be specific to DM1 (Di Costanzo et al., 2001), although other genetic disorders, such as cerebral autosomal dominant arteriopathy with subcortical infarcts and leukoencephalopathy (CADASIL) and cerebral autosomal recessive arteriopathy with subcortical infarcts and leukoencephalopathy (CARASIL) are characterised by T2-weighted hyperintensities, which, particularly at the onset of the disease, tend to localise to the anterior temporal lobes (Liem et al., 2008; Kim et al., 2018). Whether the origin of this particular class of lesions differs from that of the others in DM1 remains to be determined. In addition to macroscopic lesions, advanced MRI techniques, such as diffusion tensor imaging, provided evidence for subtle white matter changes throughout the DM1 brain (Minnerop et al., 2011; Serra et al., 2015).

The substrate of macroscopic lesions and microscopic damage in DM1 remains unknown, although axonal loss and demyelination have been reported to occur, together with gliosis (Mondelli et al., 1993; Vielhaber et al., 2006). Tackling the origin of the widespread brain damage observed in DM1 and its link with the severity of the genetic load (Serra et al., 2015), is paramount in order to understand the pathogenesis of central nervous system symptoms in DM1 and develop appropriate interventions. Although a detailed answer to these questions can only be achieved with histopathology, quantitative MRI provides a useful tool for investigating lesion characteristics in vivo. The purpose of the current study was thus to compare the lesion distribution, and its substrate (as assessed by quantitative MRI) with another condition characterised by spatially disseminated lesions with mixed pathology, namely MS. MS is a chronic inflammatory disorder of the central nervous system characterised by focal lesions, pathologically explained by a variable combination of demyelination, inflammation, axonal damage and gliosis (Filippi et al., 2001; Kutzelnigg et al., 2005; Frischer et al., 2009; Popescu and Lucchinetti, 2012; Spanò et al., 2018). Microscopic tissue abnormalities are known to occur outside macroscopic lesions, in the so-called normal-appearing white matter (NAWM) since very early clinical stages (Raz et al., 2010). The rationale for this comparison was to use MS as a pathological model, against which to compare DM1. One of the reasons for choosing MS, is that it has been studied extensively using quantitative MRI techniques, including diffusion MRI and magnetization transfer (MT) MRI. MT imaging exploits the interaction between those protons embedded in macromolecular structures (proteins and lipids) and those in free water to indirectly measure the density of the former protons (Wolff and Balaban, 1989). This allows an indirect quantification of the myelin content, given the assumption that myelin is the predominant macromolecule in the central nervous system (Heath et al., 2018). The most commonly used approach to quantify the MT effects is the so called MTR or MT-ratio, which is computed as a percentage difference between 2 images, one using off-resonance saturation (which sensitizes only macromolecules) and one without (Helms et al., 2008). Pathological changes appear to reduce the density of macromolecules and their exchange of magnetization with the free protons, thus causing a reduction of the MT ratio (Wolff and Balaban, 1989). The MTR, however, is a simplistic approach, highly dependent on the acquisition parameters, and with limited sensitivity. In order to overcome some of these limitations, more complex analytical models have been developed to provide a truly 'quantitative' estimation of myelin in the examined image (Henkelman et al., 1993). Quantitative magnetization transfer (qMT) uses multiple off-resonance frequencies and radiofrequency amplitudes to fit an analytical model of the signal, thus enabling the estimation of the pool size ratio, or F. The use of F as a proxy for myelin density has been validated in MS using post-mortem samples (Schmierer et al., 2007) and animal models of demyelination and remyelination (Turati et al., 2015).

Against this background, we set out to compare the myelin density (by means of F) in the brain of patients with DM1 to healthy controls and to patients with MS as a prototypical disorder of myelin. We first characterised the spatial distribution of lesions, and then quantified the qMT parameters inside and outside macroscopic lesions. Finally, we isolated temporal lobe lesions in patients with DM1, with the aim to test whether their qMT parameters differ from those computed in the lesions detected in the rest of the brain. Based on the existing literature, we expected DM1 patients to have more white matter lesions than healthy controls, with evidence of demyelination (Abe et al., 1994; Mizukami et al., 1999). However, we hypothesised that the extent of demyelination would be lower in DM1 than MS. Finally, while the anterior temporal pole might be involved in progressive forms of MS, we did not expect anterior temporal lesions to be a prominent feature of patients with relapsing remitting MS, included in this study. Therefore, we postulated that anteroior temporal lesions would be detecetd in DM1 only, and would have different characteristics than other lesions.

## 2. Methods

### 2.1. Participants

We recruited 28 patients (M/F = 14/14; mean age: 42, standard deviation: 12.1 years) with a molecular diagnosis of DM1 from the Neuromuscular and Neurological Rare Diseases Center at San Camillo Forlanini Hospital (Rome, Italy) and the Institute of Neurology at the Catholic University of Rome (Rome, Italy). A subsample of this cohort also participated in an independent study (Serra et al., 2015) but their qMT data have not been reported elsewhere. The genetic and clinical characteristics of DM1 patients are summarized in Table 1. Twenty-nine patients (M/F = 11/18; mean age: 35, standard deviation: 7.64 years) with a clinically definite diagnosis of relapsing remitting MS, as defined by 2001 McDonald criteria (McDonald et al., 2001) were recruited as the MS control group, from the specialist MS outpatient clinic at IRCCS Santa Lucia Foundation, Rome, Italy. All patients had a diagnosis of relapsing-remitting MS, and those who had any relapse or corticosteroid treatment over the 3 months preceding MR acquisition were excluded. DM1 participants had assessment of CTG expansion size within the DMPK gene, and they were classified according to the International Myotonic Dystrophy Consortium nomenclature (IDMC,

**Table 1**
Principal clinical and genetic characteristics of DM1 patients.

| Characteristic | No (%) of patients |
|---|---|
| *Age at onset* | |
| Childhood (age range 6–17 years) | 8 (29) |
| Adulthood (age range, 18–60 years) | 20 (71) |
| No of CTG triplet repeats on DMPK gene, mean (SD) [range] | 469.85 (311.6) [54–1200] |
| *Expansion group* | |
| E1 (50–150) | 4 (14%) |
| E2(151–500) | 13 (46%) |
| E3 (501–1000) | 9 (32%) |
| E4 (>1000) | 2 (7%) |
| *MIRS score* | |
| 1 | 4 (14%) |
| 2 | 8 (29%) |
| 3 | 12 (43%) |
| 4 | 4 (14%) |
| 5 | 0 |

Abbreviations: DM1: myotonic dystrophy type 1; DMPK: myotonic dystrophy protein kinase; MIRS: Muscular Impairment Rating Scale.

2000). Fifteen healthy controls (M/F = 7/8; mean age: 33, standard deviation: 8.4 years) were recruited through classified advertisements. This study received ethical approval from the ethical committee of the IRCCS Santa Lucia Foundation, Rome, Italy. Written informed consent was obtained from all participants before study initiation.

### 2.2. Genetic assessment

Blood samples were taken from DM1 patients to detect expanded alleles. As previously described (Serra et al., 2015), the analysis of normal and proto-mutated alleles was done using "touch down" PCR on DNA extracted from peripheral blood leucocytes (PBL). This required 50 pg of PBL-DNA being amplified in a 20 μl volume with fluorescent labelled primer 101 and primer 102. Eight rounds of reactions were cycled at 94 °C-30", 68 °C-30" (−1 °C per cycle) and 72 °C-30", followed by 30 rounds at 94 °C-30", 60 °C- and 72 °C -30". Abi-Prism 310 Genetic Analyzer was then used to analyse PCR products. Determination of expanded alleles was performed on 10 pg of PBL DNA, which underwent XL-PCR and 1% agarose gel electrophoresis. Southern blotting with subsequent hybridization to a 32P radiolabelled (CTG) 7 oligonucleotide probe was then used to analyse PCR products followed by detection using autoradiography.

### 2.3. MRI acquisition

All patients and healthy controls received an MRI scan, obtained using a head-only 3.0 T scanner (Siemens Magnetom Allegra, Siemens Medical Solutions, Erlangen, Germany), equipped with a circularly polarised transmit–receive coil. The maximum gradient strength is 40 $mTm^{-1}$, with a maximum slew rate of 400 $mTm^{-1}ms^{-1}$. The MRI session included for every subject: (1) a dual-echo turbo spin echo (TSE) (TE1 = 12 ms; TE2 = 109 ms; TR = 6190 ms; ETL = 5, matrix = 256 × 192; FOV = 230 × 172.5 $mm^2$; slice thickness = 3 mm; total number of slices = 48); (2) a fluid attenuated inversion recovery (FLAIR) scan (TE = 96 ms; TR = 8170 ms; TI = 2100 ms;ETL = 13; same matrix and FOV as the dual echo; slice thickness = 3 mm, total number of slices = 45); (3) a magnetization prepared rapid gradient echo (MPrage) sequence (TE = 2.74 ms; TR = 2500 ms; TI = 900; flip angle = 88°; matrix = 256 × 208 × 176; FOV = 256 × 208 × 176 $mm^3$); (4) a series of 12 MT-weighted 3D fast low-angle shot (FLASH) sequences (TE = 7.4 ms; TR = 35 ms; flip angle = 78; matrix = 128 × 96 × 28; FOV = 230 × 172.5 × 140 $mm^3$), optimised for qMT (Cercignani & Alexander, 2006; Cercignani et al., 2009); (5) three 3D FLASH sequences with three different flip angles were collected for mapping the observed T1 of the system (TE = 4.8 ms, TR = 15 ms, flip angles = 5, 7, 15°, respectively, same matrix and FOV as the MT sequence) and (6) three 3D FLASH sequences with near-180 flip angles were collected for B1mapping (TE = 4.8 ms, TR = 28 ms, flip angles = 155°, 180°, 205°, respectively, matrix = 64 × 64 × 40, FOV = 220 × 220 × 160 $mm^3$). The total scan time was approximately 40 min.

### 2.4. Lesion contouring and lesion masks

The volume of white matter lesions was assessed using a semi-automated local thresholding contouring software (Jim, Version 7, Xinapse Systems, Colchester, UK; www.xinapse.com) on FLAIR scans. Dual-echo scans were used as a reference to increase confidence in lesion identification. A binary lesion mask was obtained for every subject by setting all voxels within a lesion to 1 and the background to zero. The resulting lesion masks were coregistered with every patient's MPRAGE using an affine registration in ANTs (Avants et al. 2011). Magnetization transfer data were processed using customized software that fits a binary spin bath model to the data acquired with variable settings of MT pulse offset frequency and flip angle (Cercignani et al., 2009; Giulietti et al., 2012). Among other model parameters, this process yields maps of the pool size ratio (F), computed as $F = M_0^b/M_0^a$, where $M_0^a$ represents the spin density of the liquid pool, and $M_0^b$ represents the spin density of the macromolecular pool. F expresses the relative density of macromolecules, it is unitless, and is known to correlate with myelin content (Turati et al., 2015). The MPRAGE scan was segmented into white matter, grey matter and cerebrospinal fluid (CSF) for every participant. Next, it was coregistered to the 15° volume acquired as part of sequence 5, used as a reference space for the qMT scans. The same transformation was applied to the white matter segment. A white matter mask was obtained by thresholding the result at 0.8. For all participants with lesions, a NAWM mask was obtained by subtracting the lesion mask from the white matter mask. The average F was computed within lesions and NAWM for every participant. The lesion masks were warped into MNI space and lesion probability maps were obtained for each patient group.

### 2.5. Identification of temporal lesions

FLAIR scans and lesion masks of DM1 patients were visually inspected by 2 experienced observers to identify the presence of anterior temporal lobe lesions. For patients who showed them, separate masks of temporal and non-temporal lesions were created, and F values extracted for comparison.

### 2.6. Volumetric analysis

As brain atrophy is known to occur in both, MS and DM1, we also compared some measures of global and local brain volume. Every participants' MPRAGE was segmented using SPM (Di Paola et al., 2008), after lesion filling. The grey matter, white matter and CSF probability images in standard space were 'modulated', i.e. multiplied by the jacobian of the warping transformation to preserve volumetric information. The brain parenchymal fraction (BPF) was computed as the sum of the grey and white matter volume divided by the total intracranial volume.

### 2.7. Statistical analysis

Statistical analyses on clinical and imaging data were performed using SPSS (SPSS Inc., Chicago, Illinois). The imaging data included in the analysis are: lesion load, BPF, mean lesion F, mean NAWM F values. Before analysis, data were plotted to check their distribution. Values are expressed as mean ± standard deviations (SDs), or as median ± interquartile ranges (IQRs) depending on the normal distribution of the values. Student's *t* test was used to compare the means of F of lesions between patients groups, means of NAWM F and means of BPF between the 3 groups. If significant differences in relevant cohort characteristics (e.g., age, sex) were present, multiple linear regression analysis was

used. Due to skewness in its distribution, the lesion load data was normalized using logarithmic transformation and comparison between the means of each group was carried out with Student's *t* test. Linear regressions were used to examine the relationship between the neuroimaging parameters examined and triplet expansion accounting for age.

## 3. Results

### 3.1. Demographic and clinical characteristics

The three groups did not differ significantly with regard to sex but DM1 patients in our cohort tended to be older (Mean age: 42.1; SD: 12.1 years) than MS patients (Mean age: 35.8, SD: 7.63 years), and healthy controls were younger overall, but a smaller group (Mean 33.8, SD 8.4) ($X^2$ 1.1p = ns; p = 0.009 respectively). The patients with MS had a median expanded disability status scale (EDSS) score of 2.0 (range: 0–4), and a mean disease duration of 7.7 years (SD: 4.2). Their mean number of years of formal education was 13.2 (SD: 3.5). Table 1 summarizes the principal clinical and genetic characteristics of the DM1 patients. A larger proportion of patients had adult onset DM1, 20 out of 28 (71%), while 8 out of 28 (29%) had childhood disease onset. The mean triplet expansion was 469.85, with a range of 54–1200. Each expansion was grouped according to the guidelines of the Myotonic Dystrophy consortium (IDMC, 2000).

### 3.2. Lesion burden and radiological results

As we expected, patients with MS in our cohort had more extensive white matter disease. Once normalised on the logarithmic scale, an independent *t* test demonstrated that the mean lesion volume was higher in MS (median 6386, IQR 20100) than DM1 (median 2288.8, IQR 6995.3) (p = 0.002, CI −0.717 to −0.165). The healthy control cohort did not show any macroscopic lesions. The BPF was lower in MS than in DM1 patients (p = 0.009, CI = 0.009–0.06), and higher in healthy controls than in both patient groups (p = 0.0001, CI = 0.034–0.099 for MS, and p = 0.02, CI = 0.005–0.06 for DM1).

Table 2 summarises the principal MRI characteristics of the patient groups.

Examining the lesion substrate of all patients, we found more evidence of myelin disruption within lesions compared to NAWM, with the mean F of lesions being lower than the NAWM (p < 0.01, CI 0.06–0.07), and lower in MS than in DM1 (p < 0.01, CI 0.01–0.04).

In addition to examining the lesion volume in each group, we also investigated the distribution of lesions in each cohort by creating lesion masks and probability maps. Fig. 1 shows the lesion distribution in the 2 patient groups, highlighting the overall greater lesion load in MS patients. Although the lesion volume was smaller in DM1 patients, the distribution was similar with the following exceptions: DM1 patients did not show any lesions in the cerebellum and brainstem; 3 out of 28 DM1 patients (11%) presented with a pattern of temporal lobe lesions typical for DM1 (Fig. 2). Given the small number of DM1 patients with typical temporal lesions, no formal statistical comparison was performed. A plot of the mean F and its SD for every patient is shown in Fig. 3. The data are not conclusive but suggest that F might be higher in temporal lobe compared to non-temporal lobe lesions.

Due to the differences in age and sex distribution between groups, we performed further multiple regression analyses with NAWM and lesion F, respectively, as the dependent variables, and group, age and sex as factors.

This analysis showed significant differences between F of the NAWM in the MS group compared to the DM1 (beta 0.45, p < 0.01) and control group (beta 0.42, p < 0.01), while there did not appear to be a significant difference between NAWM in DM1 patients and controls (beta −0.003, p = ns). Details are shown in Table 3.

Within lesions, multiple regression analysis indicated that patients with MS had significantly lower F compared to the DM1 cohort (beta −0.28, p < 0.01), when adjusted for age and sex as shown in Table 4.

There was no association between FLAIR lesion load, lesion F or NAWM F and either triplet expansion and age (p value > 0.5 for all models explored) in DM1 patients. The triplet expansion number was mildly correlated with patient age (p = 0.02, r = 0.43). The F of lesions in DM1 was not found to correlate to triplet expansion number (p = ns, r = 0.02). Patient age and disease onset did not demonstrate any correlation with lesion load on FLAIR (p = ns, r = 0.27, p = ns r = −0.14).

We found a statistically significant difference between lesion load in DM1 patients with adulthood and childhood onset on FLAIR once transformed to allow normalization of the data. (Adult onset: n = 20 med 3134.8 IQR 8414.75; Childhood onset: n = 8, med = 1898.2, IQR = 1857.6; p = 0.03. 95% CI 0.03 to 0.68). However, within the childhood onset group there were less patients, and the age range of this group was 18–55, with a younger median age of 32, compared to 45 (range 31–69) for the adult onset group which may explain some of this variation.

Examining for correlation between many of the clinical variables with imaging results using Spearman's and Pearson's coefficient (depending on the normality of the variable) did not demonstrate any significant correlation except for age and triplet expansion, which was mildly correlated. Given the large number of comparisons, however, this result cannot be considered conclusive.

**Table 2**
MRI measurements from DM1 and MS patients, and healthy controls.

| Characteristics | DM1 patients (n = 28) | MS patients (n = 29) | Healthy controls (n = 15) |
|---|---|---|---|
| Lesion Load on FLAIR in $mm^3$, median (IQR) [SD] | 2288 (6995) [4217] | 6386 (20100) [14879] | N/A |
| Lesion F, mean [SD] | 0.14 [0.02] | 0.12 [0.02] | N/A |
| NAWM F, mean [SD] | 0.21 [0.01] | 0.17 [0.02] | 0.22 [0.01] |
| BPF | 0.802 [0.043] | 0.767 [0.053] | 0.834 [0.040] |

Abbreviations: DM1: myotonic dystrophy type 1; FLAIR: fluid attenuated inversion recovery; MS: multiple sclerosis; NAWM: normal appearing white matter; BPF = brain parenchymal fraction.

## 4. Discussion

This study demonstrates that the white matter lesion distribution in people with DM1 largely overlaps with that typical of relapsing remitting MS, and that such lesions are likely to be characterised by demyelination, as measured by a reduction in the magnetization transfer parameter F. Conversely, no evidence of demyelination within the NAWM was observed in DM1 brains.

### 4.1. Lesion distribution

MS lesions are known to be located primarily in a perivascular distribution (Tallantyre et al., 2008). Although they can form in virtually every area of the central nervous system, their density typically increases with proximity to the ventricles, suggesting a role for CSF-mediated factors in the accumulation of damage (Jehna et al., 2015). Our results suggest that white matter lesions tend to follow a similar anatomical pattern in DM1 patients, at least in the supratentorial compartment. Whether this distribution is suggestive of similar mechanisms of lesion formation remains to be clarified. Lesion distribution in MS has been postulated to be related to lymphocyte trafficking pathways and distinct antigen presentation depending on the particular area of the central nervous system involved (Gross et al., 2017). It is likely that the mechanism is different in DM1, however an inflammatory reaction to RNA inclusion bodies may be a hypothesis to consider. Despite the similar lesion distributions in the 2 patient cohorts (i.e., DM1 and MS), there were also some important differences. First, none of the DM1 patients showed any lesions in the cerebellum and brainstem, which again remarks substantial pathophysiological differences between DM1 and

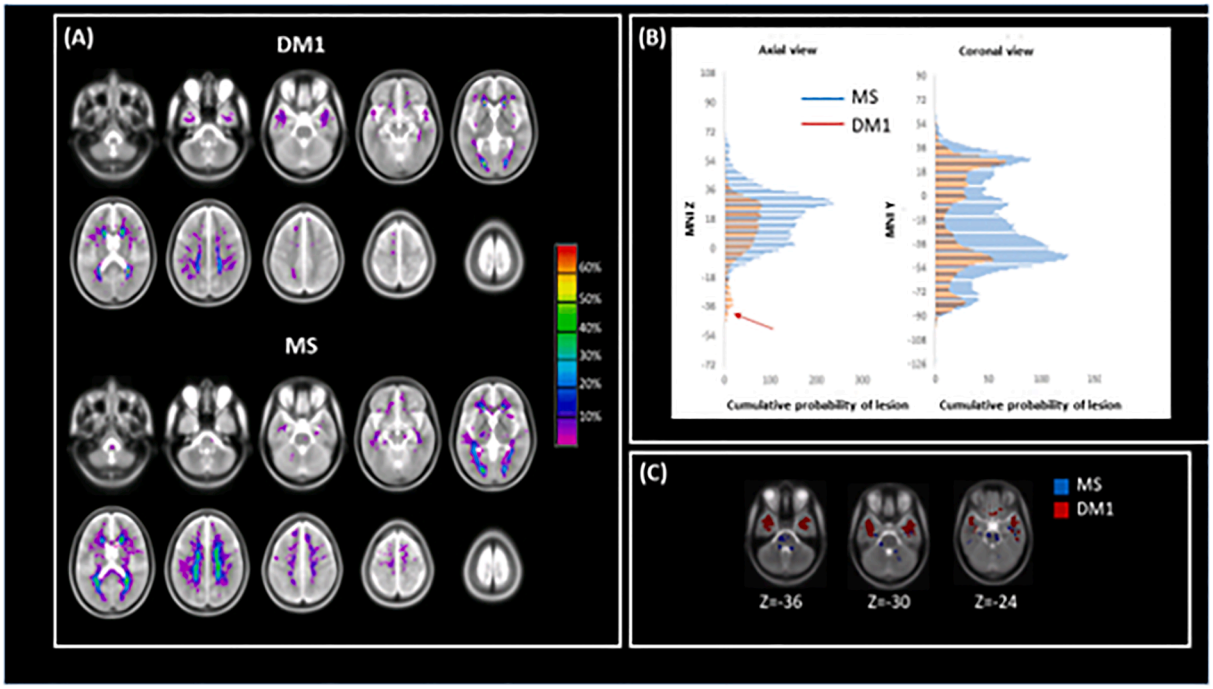


**Fig. 1.** Lesion distribution. Panel A shows the lesion probability maps for DM1 (top) and MS (bottom). Panel B shows the sum of the probabilities over each section in the axial (left) and coronal (right) planes. It can be seen that MS patients have higher probability of lesions at every level except at MNI z coordinates ranging from −40 to −20. Panel C demonstrates that in correspondence with these coordinates, DM1 patients show extensive lesions in the anterior temporal lobe, while MS patients have primarily sub-tentorial lesions, in the brainstem and cerebellum. Abbreviations: DM1: myotonic dystrophy type 1, MS: Multiple sclerosis.

MS with respect to macroscopic white matter damage. Interestingly, infratentorial lesions are common in MS, and often associated with clinical symptoms when in relation with an acute MS relapse. In addition, 3 DM1 patients (but none of the MS patients) showed the typical anterior temporal white matter lesions (Fig. 2). This is consistent with previous imaging studies of patients with DM1 demonstrating specificity for the anterior temporal region (Miaux et al., 1997; Ogata et al., 1998), whose pathological substrate has been characterized by decreased myelin sheaths and severely disordered arrangement of axons with microscopically heterotopic neurons (Ogata et al., 1998). As only 3 patients in our sample presented with anterior temporal lobe lesions, it was not possible to perform a formal statistical analysis of those patients or investigate any correlation with triplet size or a significantly larger lesion load compared to other parts of the brain. Nonetheless, these anterior temporal lesions showed (in 2 out of 3 cases) higher F values in comparison with those distributed to other brain regions. It is difficult to provide a definite interpretation of this finding. Post-mortem studies of DM1 have recognized different substrates in different areas of the brain, such as inclusion bodies in the cerebral cortex and neurofibrillary tangles in the temporal lobes, a finding which may suggest that the variation of lesion distribution being seen, could occur due to different substrate involvement (Ono et al., 1987, 1989). However, it is also possible that these differences are explained by intrinsic variations in tissue type. A similar finding, differentiating between periventricular and deep white matter hyperintensities in an aging cohort was interpreted as evidence of altered fluid dynamic and CSF leakage in the periventricular area, possibly linked to abnormal glymphatic system function (Iordanishvili et al., 2019). Although this is an intriguing hypothesis, given the small number of anterotemporal lesions in this study, we refrain from speculating on this subject. Considering the questions remaining regarding the mechanisms of disease, in future research, it may be important to compare DM1 with other genetically inherited neurological disorders, which predominantly affect white matter, through imaging and histological studies. CADASIL is an arteriopathy which results in white matter disease, predominantly in the anterior temporal lobes due to vascular insult (Liem et al., 2008). Mitochondrial neurogastrointestinal encephalopathy (MNGIE) is a rare autosomal recessive disorder caused by mutations in the thymidine phosphorylase gene, which leads to excess levels of thymidine and resultant mitochondrial DNA replication abnormalities. A study by Gramegna et al. found evidence of microvascular damage leading to diffuse white matter involvement in patients with MNGIE on brain MRI, MR spectroscopy and histopathology (Gramegna et al., 2018a). Additionally, another interesting observation by the same group has highlighted the potential role of mitochondrial dysfunction in DM1, illustrating that patients with higher levels of CSF lactate on MR spectroscopy also demonstrate greater white matter disease (Gramegna et al., 2018b). Comparing these disease entities using advanced neuroimaging techniques alongside histopathology could shed further light on the disease mechanisms involved in DM1.

### 4.2. Lesion substrate

With regards to the quantitative analysis, we demonstrate that, while we found no evidence of demyelination in the NAWM of DM1 patients in our study, F values within the lesions are significantly reduced, suggesting a reduction in myelin density. It should be reiterated, however, that F is computed as a ratio, and therefore a reduction could be caused by either, a decrease in the numerator, or an increase in the denominator. The latter could happen in the presence of oedema (i.e., an increase in free water). Indeed, previous experimental studies have demonstrated that inflammation in the absence of demyelination can cause similar changes (Stanisz et al., 2004). Therefore this study cannot conclude with absolute certainty that demyelination explains all the observed changes in F from DM1 brains. The average F values from DM1 lesions are higher than MS lesions, suggesting a less extensive loss of myelin, but they are significantly lower than in the NAWM, and than in the white matter of healthy controls. Neuropathological investigations in DM1 are extremely limited (Ogata et al., 1998; Mizukami et al., 1999; Itoh et al., 2010). Itoh et al. (2010) who examined 11 patients with DM1

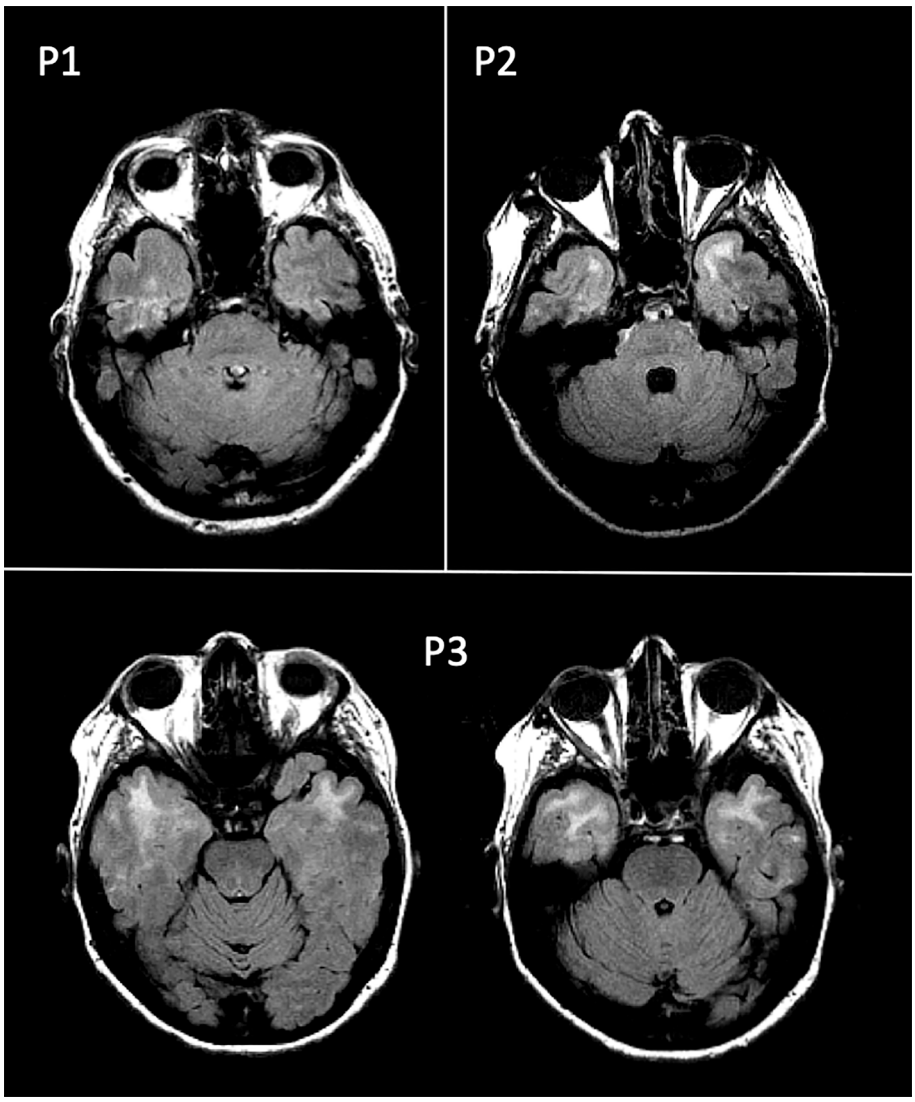


**Fig. 2.** Axial sections of the fluid-attenuated inversion recovery (FLAIR) scans, showing the anterior temporal lesions observed in 3 patients with myotonic dystrophy type 1 (P1, P2, P3).

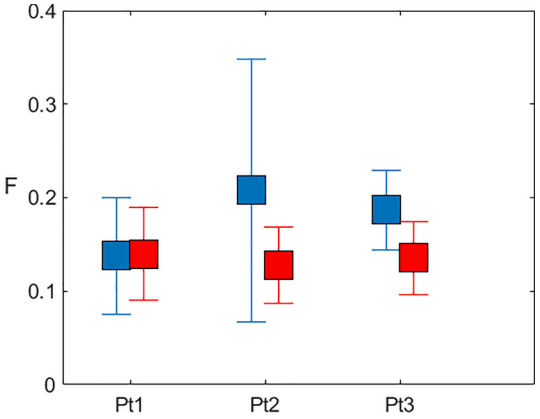


**Fig. 3.** Mean (SD) F value in temporal (blue) and non-temporal (red) lesions, for the 3 patients with myotonic dystrophy type 1 who presented with anterior temporal lobe lesions. (For interpretation of the references to colour in this figure legend, the reader is referred to the web version of this article.)

**Table 3**
Summary of Multiple Regression analysis for model examining difference in variances of NAWM F values in MS compared to DM1 patients and healthy controls adjusted for age and sex.

| Variable | ℓ | P value | Confidence interval |
|---|---|---|---|
| Intercept | 0.225 | | |
| DM1 | 0.45 | <0.001 | 0.033 to 0.057 |
| Control | 0.42 | <0.001 | 0.028 to 0.055 |
| Age | 0.00 | 0.858 | 0.0 to 0.0 |
| Sex | −0.011 | 0.013 | −0.019 to −0.002 |

Abbreviations: DM1: myotonic dystrophy type 1; MS: multiple sclerosis; NAWM: normal appearing white matter.

reported, in the deep white matter, microscopic evidence of dilated perivascular spaces, loss of adjacent axons and myelin, capillary hyalinization, and fibrillary gliosis. They argued that the macroscopic lesions detectable on MRI scans in the white matter of DM1 patients may be considered as instances of état criblé and represent a DM1 specific morphological change. Interestingly, they did not report any obvious abnormality in the NAWM, consistently with our current results.

Although MTR has been used previously to investigate brain changes occurring in DM1, this is the first study to use qMT. It is important to

**Table 4**
Summary of Multiple Regression analysis for model examining differences in variances of F value of lesions in MS and DM1, adjusted for age and sex.

| Variable | 6 | P value | Confidence interval |
|---|---|---|---|
| Intercept | 0.141 | 0.00 | 0.109 to 0.173 |
| DM1 | 0.28 | <0.01 | 0.012 to 0.043 |
| MS | −0.28 | <0.01 | −0.040 to −0.012 |
| Age | 0.00 | 0.882 | −0.001 to 0.001 |
| Sex | 0.003 | 0.71 | −0.012 to 0.017 |

Abbreviations: DM1: myotonic dystrophy type 1; MS: multiple sclerosis.

reiterate that this technique provides a more specific quantification of myelin than MTR, as the MTR is acquisition-dependent and incorporates effects independent of myelin content (Cercignani & Bouyagoub, 2018), such as changes in T1 (Henkelman et al., 2001) and changes in extracellular volume fraction (Stanisz et al., 2004). This might explain why a previous investigation of NAWM in DM1 using MTR found significant differences between DM1 patients and healthy controls (Naka et al., 2002) while we did not. It is possible that the changes observed by Naka et al. (2002) are explained by substrates other than demyelination. An additional difficulty in comparing results of studies in this patient cohort rests on the small numbers often included, the significant effects of anticipation and expansion number on phenotype, the variation in group onset and in imaging protocols, some or all of which may help explain the difference in results with respect to the NAWM. Our findings are consistent with other studies demonstrating reduced F value within lesions in MS, in terms of the values of the lesions' substrate (Sled 2018). As qMT is a relatively novel technique, not available on clinical scanners, it is difficult to find studies that have applied it to diseases such as CADASIL, which would be very helpful to compare against our current findings.

### 4.3. Correlation with clinical and genetic data

Our results did not demonstrate any correlation between triplet number and lesion load, F value or MIRS(Muscular impairment rating scale) scores. There has been reported variability between triplet size depending on the site at which it is sampled, for example, repeats are larger in muscle samples than in corresponding blood samples (Thornton et al., 1994). In clinical practice samples are always taken from the blood, however it is possible that CSF samples might more accurately reflect increasing lesion load or changes in the central nervous system, and this may be something to consider in future studies. Different studies have demonstrated varied results with regards to correlation between MRI changes, clinical findings, cognition, and triplet expansion (Meola and Sansone, 2007; Serra et al., 2015). This disparity again may result from the well-known heterogeneity within this patient group due to differences in genetic inheritance and expression, clinical phenotypes, and notably study designs. It has been shown that modal CTG repeat length might not be the best variable to consider for these correlations, as it tends to correlate with the age of onset (Cumming et al., 2019). Instead, progenitor CTG repeat length is the best predictor of risk severity and the best index to correlate with clinical or neuroimaging findings (Cumming et al., 2019; Morales et al., 2020). This information was not available for this study and we have tried to mitigate the problem by accounting for age of particiapants. However, this should be regarded as a limitation.

### 4.4. Limitations

This study has other limitations; our sample size is small, which is in keeping with DM1 being a relatively rare disease. The DM1 cohort is smaller again, once divided into adult and childhood onset. Differences of disease onset may demonstrate more significant differences in a larger cohort. It is well known that patients with DM1 experience genetic anticipation, with earlier symptomatic and more severe disease in families who have had successive affected generations (Höweler et al., 1989). We could not examine whether the prevalence of white matter disease is greater in those patients with a more significant family history. In addition to this, despite our relatively young cohort of DM1 patients, they were significantly older than both the MS cohort and healthy controls. With regards to this, it would be useful to examine the effect of disease duration and age on the extent of white matter disease, which is something that could be considered in future studies. A further point of interest might have been to examine whether the participants had inherited DM1 from the maternal or paternal line. Martorell et al. suggested that patients with paternal inheritance can exhibit low numbers of triplet expansions while those with maternally inherited disease are more likely to suffer from clinically significant disease (Martorell et al, 2001; Martorell et al., 2007). The existence of co-morbidities such as ischaemic heart disease, hypertension and smoking, which may be present in DM1 as in the general population, may also contribute to white matter disease but these variables were not examined in this study. They are variables which may be useful to be aware of in future studies. Finally, we have not included patients with congenital or late DM1 clinical onset . Future studies comparing lesion distribution and load in these subgroups of patients is an area which may add further weight to the specificity of DM1 lesions to the temporal lobes and the nature of white matter changes.

### 4.5. Conclusion

In conclusion, we have shown that the distribution of lesions within the white matter is similar in DM1 and MS, suggesting that proximity to the ventricles might increase susceptibility to tissue damage regardless of the underlying pathological mechanism. In addition, we have demonstrated that demyelination occurs within DM1 lesions, but not in the NAWM, and that the DM1 typical anterior temporal lesions might be different from the periventricular ones. These data support the use of quantitative MRI techniques for the characterization of brain changes associated with DM1, and the need for sensitive non-invasive imaging biomarkers to aid in our monitoring of progression, possible response to treatment and advancing our understanding of this disease.

## Declaration of Competing Interest

The authors declare no competing financial interests.

## Acknowledgments

This work was funded in part by a grant from the Italian Ministry of Health (RF-2013 02358409) awarded to M. Cercignani. G. Meola is supported by FMM-Fondazione Malattie Miotoniche-Milan, Italy.

## References

Abe, K., Fujimura, H., Toyooka, K., Yorifuji, S., Nishikawa, Y., Hazama, T., Yanagihara, T., 1994. Involvement of the central nervous system in myotonic dystrophy. J. Neurol. Sci. 127, 179–185. https://doi.org/10.1016/0022-510X(94)90071-X.

Abe, K., Fujimura, H., Soga, F., 1998. The fluid-attenuated inversion-recovery pulse sequence in assessment of central nervous system involvement in myotonic dystrophy. Neuroradiology 40, 32–35. https://doi.org/10.1007/s002340050534.

Ashizawa, T., Gagnon, C., Groh, W.J., Gutmann, L., Johnson, N.E., Meola, G., Moxley, R., Pandya, S., Rogers, M.T., Simpson, E., Angeard, N., Bassez, G., Berggren, K.N., Bhakta, D., Bozzali, M., Broderick, A., Byrne, J.L.B., Campbell, C., Cup, E., Day, J.W., De Mattia, E., Duboc, D., Duong, T., Eichinger, K., Ekstrom, A.-B., van Engelen, B., Esparis, B., Eymard, B., Ferschl, M., Gadalla, S.M., Gallais, B., Goodglick, T., Heatwole, C., Hilbert, J., Holland, V., Kierkegaard, M., Koopman, W.J., Lane, K., Maas, D., Mankodi, A., Mathews, K.D., Monckton, D.G., Moser, D., Nazarian, S., Nguyen, L., Nopoulos, P., Petty, R., Phetteplace, J., Puymirat, J., Raman, S., Richer, L., Roma, E., Sampson, J., Sansone, V., Schoser, B., Sterling, L., Statland, J., Subramony, S.H., Tian, C., Trujillo, C., Tomaselli, G., Turner, C., Venance, S., Verma, A., White, M., Winblad, S., 2018. Consensus-based care recommendations for

adults with myotonic dystrophy type 1. Neurol. Clin. Pract. 8, 507–520. https://doi.org/10.1212/CPJ.0000000000000531.
Avants, B.B., Tustison, N.J., Song, G., Cook, P.A., Klein, A., Gee, J.C., 2011. A reproducible evaluation of ANTs similarity metric performance in brain image registration. Neuroimage 54, 2033–2044. https://doi.org/10.1016/j.neuroimage.2010.09.025.
Brook, J.D., McCurrach, M.E., Harley, H.G., Buckler, A.J., Church, D., Aburatani, H., Hunter, K., Stanton, V.P., Thirion, J.-P., Hudson, T., Sohn, R., Zemelman, B., Snell, R. G., Rundle, S.A., Crow, S., Davies, J., Shelbourne, P., Buxton, J., Jones, C., Juvonen, V., Johnson, K., Harper, P.S., Shaw, D.J., Housman, D.E., 1992. Molecular basis of myotonic dystrophy: expansion of a trinucleotide (CTG) repeat at the 3' end of a transcript encoding a protein kinase family member. Cell 68, 799–808. https://doi.org/10.1016/0092-8674(92)90154-5.
Caso, F., Agosta, F., Peric, S., Rakočević-Stojanović, V., Copetti, M., Kostic, V.S., Filippi, M., Kassubek, J., 2014. Cognitive impairment in myotonic dystrophy type 1 is associated with white matter damage. PLoS One 9, e104697. https://doi.org/10.1371/journal.pone.0104697.
Cercignani, M., Alexander, D.C., 2006. Optimal acquisition schemes for in vivo quantitative magnetization transfer MRI. Magn. Reson. Med. 56, 803–810. https://doi.org/10.1002/mrm.21003.
Cercignani, M., Basile, B., Spanò, B., Comanducci, G., Fasano, F., Caltagirone, C., Nocentini, U., Bozzali, M., 2009. Investigation of quantitative magnetisation transfer parameters of lesions and normal appearing white matter in multiple sclerosis. NMR Biomed. 22, 646–653. https://doi.org/10.1002/nbm.1379.
Cercignani, M., Bouyagoub, S., 2018. Brain microstructure by multi-modal MRI: Is the whole greater than the sum of its parts? Neuroimage 182, 117–127. https://doi.org/10.1016/j.neuroimage.2017.10.052.
Cumming, S.A., Jimenez-Moreno, C., Okkersen, K., Wenninger, S., Daidj, F., Hogarth, F., Littleford, R., Gorman, G., Bassez, G., Schoser, B., Lochmüller, H., van Engelen, B.G. M., Monckton, D.G., 2019. Genetic determinants of disease severity in the myotonic dystrophy type 1 OPTIMISTIC cohort. Neurology 93, e995–e1009. https://doi.org/10.1212/WNL.0000000000008056.
Damian, M.S., Schilling, G., Bachmann, G., Simon, C., Stöppler, S., Dorndorf, W., 1994. White matter lesions and cognitive deficits: relevance of lesion pattern? Acta Neurol. Scand. 90, 430–436. https://doi.org/10.1111/j.1600-0404.1994.tb02753.x.
Di Costanzo, A., Di Salle, F., Santoro, L., Bonavita, V., Tedeschi, G., 2001. Dilated Virchow-Robin spaces in myotonic dystrophy: frequency, extent and significance. Eur. Neurol. 46, 131–139. https://doi.org/10.1159/000050786.
Di Costanzo, A., Di Salle, F., Santoro, L., Tessitore, A., Bonavita, V., Tedesch, i.G., 2002. Pattern and significance of white matter abnormalities in myotonic dystrophy type 1: an MRI study. J. Neurol. 249, 1175–1182. https://doi.org/10.1007/s00415-002-0796-z.
Di Paola, M., Bozzali, M., Fadda, L., Musicco, M., Sabatini, U., Caltagirone, C., 2008. Reduced oxygen due to high-altitude exposure relates to atrophy in motor-function brain areas. Eur. J. Neurol. 15, 1050–1057. https://doi.org/10.1111/j.1468-1331.2008.02243.x.
Emery, A.E.H., 1991. Population frequencies of inherited neuromuscular diseases – a world survey. Neuromuscul. Disord. 1, 19–29. https://doi.org/10.1016/0960-8966(91)90039-U.
Fernandez, R.E., Rothberg, M., Ferencz, G., Wujack, D., 1990. Lyme disease of the CNS: MR imaging findings in 14 cases. AJNR Am. J. Neuroradiol. 11, 479–481.
Filippi, M., Bozzali, M., Comi, G., 2001. Magnetization transfer and diffusion tensor MR imaging of basal ganglia from patients with multiple sclerosis. J. Neurol. Sci. 183, 69–72. https://doi.org/10.1016/S0022-510X(00)00471-8.
Frischer, J.M., Bramow, S., Dal-Bianco, A., Lucchinetti, C.F., Rauschka, H., Schmidbauer, M., Laursen, H., Sorensen, P.S., Lassmann, H., 2009. The relation between inflammation and neurodegeneration in multiple sclerosis brains. Brain 132, 1175–1189. https://doi.org/10.1093/brain/awp070.
Fu, Y.H., Friedman, D.L., Richards, S., Pearlman, J.A., Gibbs, R.A., Pizzuti, A., Ashizawa, T., Perryman, M.B., Scarlato, G., Fenwick, R.G., Caskeyt, C.T., 1993. Decreased expression of myotonin-protein kinase messenger RNA and protein in adult form of myotonic dystrophy. Science 260, 235–238. https://doi.org/10.1126/science.8469976. PMID: 8469976.
Giulietti, G., Bozzali, M., Figura, V., Spanò, B., Perri, R., Marra, C., Lacidogna, G., Giubilei, F., Caltagirone, C., Cercignani, M., 2012. Quantitative magnetization transfer provides information complementary to grey matter atrophy in Alzheimer's disease brains. Neuroimage 59, 1114–1122. https://doi.org/10.1016/j.neuroimage.2011.09.043.
Glantz, R.H., Wright, R.B., Huckman, M.S., Garron, D.C., Siegel, I.M., 1988. Central nervous system magnetic resonance imaging findings in myotonic dystrophy. Arch. Neurol. 45, 36–37. https://doi.org/10.1001/archneur.1988.00520250042017.
Gramegna, L.L., Giannoccaro, M.P., Manners, D.N., Testa, C., Zanigni, S., Evangelisti, S., Bianchini, C., Oppi, F., Poda, R., Avoni, P., Lodi, R., Liguori, R., Tonon, C., 2018b. Mitochondrial dysfunction in myotonic dystrophy type 1. Neuromuscul. Disord. 28, 144–149. https://doi.org/10.1016/j.nmd.2017.10.007.
Gramegna, L.L., Pisano, A., Testa, C., Manners, D.N., D'Angelo, R., Boschetti, E., Giancola, F., Pironi, L., Caporali, L., Capristo, M., Valentino, M.L., Plazzi, G., Casali, C., Dotti, M.T., Cenacchi, G., Hirano, M., Giordano, C., Parchi, P., Rinaldi, R., De Giorgio, R., Lodi, R., Carelli, V., Tonon, C., 2018a. Cerebral mitochondrial microangiopathy leads to leukoencephalopathy in mitochondrial neurogastrointestinal encephalopathy. AJNR Am. J. Neuroradiol. 39, 427–434. https://doi.org/10.3174/ajnr.A5507.
Gross, C.C., Schulte-Mecklenbeck, A., Hanning, U., Posevitz-Fejfár, A., Korsukewitz, C., Schwab, N., Meuth, S.G., Wiendl, H., Klotz, L., 2017. Distinct pattern of lesion distribution in multiple sclerosis is associated with different circulating T-helper and helper-like innate lymphoid cell subsets. Mult. Scler. 23, 1025–1030. https://doi.org/10.1177/1352458516662726.
Heath, F., Hurley, S.A., Johansen-Berg, H., Sampaio-Baptista, C., 2018. Advances in noninvasive myelin imaging. Dev. Neurobiol. 78, 136–151. https://doi.org/10.1002/dneu.22552.
Helms, G., Dathe, H., Kallenberg, K., Dechent, P., 2008. High-resolution maps of magnetization transfer with inherent correction for RF inhomogeneity and T1 relaxation obtained from 3D FLASH MRI. Magn. Reson. Med. 60, 1396–1407. https://doi.org/10.1002/mrm.21732.
Henkelman, R.M., Huang, X., Xiang, Q.-S., Stanisz, G.J., Swanson, S.D., Bronskill, M.J., 1993. Quantitative interpretation of magnetization transfer. Magn. Reson. Med. 29, 759–766. https://doi.org/10.1002/mrm.1910290607.
Henkelman, R.M., Stanisz, G.J., Graham, S.J., 2001. Magnetization transfer in MRI: a review. NMR Biomed. 14, 57–64. https://doi.org/10.1002/nbm.683.
Höweler, C.J., Busch, H.F., Geraedts, J.P., Niermeijer, M.F., Staal, A., 1989. Anticipation in myotonic dystrophy: fact or fiction? Brain 112, 779–797. https://doi.org/10.1093/brain/112.3.779.
Huber, S.J., Kissel, J.T., Shuttleworth, E.C., Chakeres, D.W., Clapp, L.E., Brogan, M.A., 1989. Magnetic resonance imaging and clinical correlates of intellectual impairment in myotonic dystrophy. Arch. Neurol. 46, 536–540. https://doi.org/10.1001/archneur.1989.00520410070026.
Hund, E., Jansen, O., Koch, M.C., Ricker, K., Fogel, W., Niedermaier, N., Otto, M., Kuhn, E., Meinck, H.M., 1997. Proximal myotonic myopathy with MRI white matter abnormalities of the brain. Neurology 1997, 33–37. https://doi.org/10.1212/wnl.48.1.33.
(IDMC), T.I.M.D.C., 2000. New nomenclature and DNA testing guidelines for myotonic dystrophy type 1 (DM1). The International Myotonic Dystrophy Consortium (IDMC). Neurology 54, 1218-1221. DOI:10.1212/wnl.54.6.1218.
Iordanishvili, E., Schall, M., Loução, R., Zimmermann, M., Kotetishvili, K., Shah, N.J., Oros-Peusquens, A.-M., 2019. Quantitative MRI of cerebral white matter hyperintensities: a new approach towards understanding the underlying pathology. Neuroimage 202, 116077. https://doi.org/10.1016/j.neuroimage.2019.116077.
Itoh, K., Mitani, M., Kawamoto, K., Futamura, N., Funakawa, I., Jinnai, K., Fushiki, S., 2010. Neuropathology does not correlate with regional differences in the extent of expansion of CTG repeats in the brain with myotonic dystrophy type 1. Acta Histochem. Cytochem. 43, 149–156. https://doi.org/10.1267/ahc.10019.
Jehna, M., Pirpamer, L., Khalil, M., Fuchs, S., Ropele, S., Langkammer, C., Pichler, A., Stulnig, F., Deutschmann, H., Fazekas, F., Enzinger, C., 2015. Periventricular lesions correlate with cortical thinning in multiple sclerosis: cortical thinning and periventricular lesions in MS. Ann. Neurol. 78, 530–539. https://doi.org/10.1002/ana.24461.
Jiang, H., Mankodi, A., Swanson, M.S., Moxley, R.T., Thornton, C.A., 2004. Myotonic dystrophy type 1 is associated with nuclear foci of mutant RNA, sequestration of muscleblind proteins and deregulated alternative splicing in neurons. Hum. Mol. Genet. 13, 3079–3088. https://doi.org/10.1093/hmg/ddh327.
Kieslich, M., Errazuriz, G., Posselt, H.G., Moeller-Hartmann, W., Zanella, F., Boehles, H., 2001. Brain white-matter lesions in celiac disease: a prospective study of 75 diet-treated patients. Pediatrics 108, e21. https://doi.org/10.1542/peds.108.2.e21.
Kim, H., Lim, Y.-M., Oh, Y.J., Lee, E.-J., Kim, K.-K., Chen, X., 2018. Comparison of brain magnetic resonance imaging between myotonic dystrophy type 1 and cerebral autosomal dominant arteriopathy with subcortical infarcts and leukoencephalopathy. PLoS One 13, e0208620. https://doi.org/10.1371/journal.pone.0208620.
Kutzelnigg, A., Lucchinetti, C.F., Stadelmann, C., Brück, W., Rauschka, H., Bergmann, M., Schmidbauer, M., Parisi, J.E., Lassmann, H., 2005. Cortical demyelination and diffuse white matter injury in multiple sclerosis. Brain 128, 2705–2712. https://doi.org/10.1093/brain/awh641.
Liem, M.K., Lesnik Oberstein, S.A.J., Haan, J., van der Neut, I.L., van den Boom, R., Ferrari, M.D., van Buchem, M.A., van der Grond, J., 2008. Cerebral autosomal dominant arteriopathy with subcortical infarcts and leukoencephalopathy: progression of MR abnormalities in prospective 7-year follow-up study. Radiology 249, 964–971. https://doi.org/10.1148/radiol.2492080357.
Mahadevan, M.S., Amemiya, C., Jansen, G., Sabourin, L., Baird, S., Neville, C.E., Wormskamp, N., Segers, B., Batzer, M., Lamerdin, J., de Jong, P., Wieringa, Bé, Korneluk, R.G., 1993. Structure and genomic sequence of the myotonic dystrophy (DM kinase) gene. Hum. Mol. Genet. 2, 299–304. https://doi.org/10.1093/hmg/2.3.299.
Martorell, L., Cobo, A.M., Baiget, M., Naudó, M., Poza, J.José., Parra, J., 2007. Prenatal diagnosis in myotonic dystrophy type 1. Thirteen years of experience: implications for reproductive counselling in DM1 families. Prenat Diagn. 27, 68–72. https://doi.org/10.1002/pd.1627.
Martorell, L., Monckton, D.G., Sanchez, A., Lopez de Munain, A., Baiget, M., 2001. Frequency and stability of the myotonic dystrophy type 1 premutation. Neurology 56, 328–335. https://doi.org/10.1212/WNL.56.3.328.
McDonald, W.I., Compston, A., Edan, G., Goodkin, D., Hartung, H.-P., Lublin, F.D., McFarland, H.F., Paty, D.W., Polman, C.H., Reingold, S.C., Sandberg-Wollheim, M., Sibley, W., Thompson, A., Van Den Noort, S., Weinshenker, B.Y., Wolinsky, J.S., 2001. Recommended diagnostic criteria for multiple sclerosis: guidelines from the International Panel on the diagnosis of multiple sclerosis. Ann. Neurol. 50, 121–127. https://doi.org/10.1002/ana.1032.
Meola, G., Cardani, R., 2015. Myotonic dystrophies: an update on clinical aspects, genetic, pathology, and molecular pathomechanisms. Biochim. Biophys. Acta 1852, 594–606. https://doi.org/10.1016/j.bbadis.2014.05.019.
Meola, G., Sansone, V., Perani, D., Scarone, S., Cappa, S., Dragoni, C., Cattaneo, E., Cotelli, M., Gobbo, C., Fazio, F., Siciliano, G., Mancuso, M., Vitelli, E., Zhang, S., Krahe, R., Moxley, R.T., 2003. Executive dysfunction and avoidant personality trait

in myotonic dystrophy type 1 (DM-1) and in proximal myotonic myopathy (PROMM/DM-2). Neuromuscul. Disord. 13, 813–821. https://doi.org/10.1016/S0960-8966(03)00137-8.
Meola, G., Sansone, V., 2007. Cerebral involvement in myotonic dystrophies. Muscle Nerve 36, 294–306. https://doi.org/10.1002/mus.20800.
Miaux, Y., Chiras, J., Eymard, B., Lauriot-Prevost, M.C., Radvanyi, H., Martin-Duverneuil, N., Delaporte, C., 1997. Cranial MRI findings in myotonic dystrophy. Neuroradiology 39, 166–170. https://doi.org/10.1007/s002340050385.
Minnerop, M., Weber, B., Schoene-Bake, J.C., Roeske, S., Mirbach, S., Anspach, C., Schneider-Gold, C., Betz, R.C., Helmstaedter, C., Tittgemeyer, M., Klockgether, T., Kornblum, C., 2011. The brain in myotonic dystrophy 1 and 2: evidence for a predominant white matter disease. Brain 134, 3530–3546. https://doi.org/10.1093/brain/awr299.
Mizukami, K., Mizukami, K., Sasaki, M., Baba, A., Suzuki, T., Shiraishi, H., 1999. An autopsy case of myotonic dystrophy with mental disorders and various neuropathologic features. Psychiatry Clin. Neurosci. 53, 51–55. https://doi.org/10.1046/j.1440-1819.1999.00470.x.
Modoni, A., Silvestri, G., Pomponi, M.G., Mangiola, F., Tonali, P.A., Marra, C., 2004. Characterization of the pattern of cognitive impairment in myotonic dystrophy type 1. Arch. Neurol. 61, 1943–1947. https://doi.org/10.1001/archneur.61.12.1943.
Mondelli, M., Rossi, A., Malandrini, A., Della Porta, P., Guazzi, G.C., 1993. Axonal motor and sensory neuropathy in myotonic dystrophy. Acta Neurol. Scand. 88, 141–148. https://doi.org/10.1111/j.1600-0404.1993.tb04206.x.
Morales, F., Vásquez, M., Corrales, E., Vindas-Smith, R., Santamaría-Ulloa, C., Zhang, B., Sirito, M., Estecio, M.R., Krahe, R., Monckton, D.G., 2020. Longitudinal increases in somatic mosaicism of the expanded CTG repeat in myotonic dystrophy type 1 are associated with variation in age-at-onset. Hum. Mol. Genet. 29, 2496–2507. https://doi.org/10.1093/hmg/ddx033.
Naka, H., Imon, Y., Ohshita, T., Honjo, K., Kitamura, T., Mimori, Y., Nakamura, S., 2002. Magnetization transfer measurements of cerebral white matter in patients with myotonic dystrophy. J. Neurol. Sci. 193, 111–116. https://doi.org/10.1016/S0022-510X(01)00652-9.
Ogata, A., Terae, S., Fujita, M., Tashiro, K., 1998. Anterior temporal white matter lesions in myotonic dystrophy with intellectual impairment: an MRI and neuropathological study. Neuroradiology 40, 411–415. https://doi.org/10.1007/s002340050613.
Ono, S., Inoue, K., Mannen, T., Kanda, F., Jinnai, K., Takahashi, K., 1987. Neuropathological changes of the brain in myotonic dystrophy–some new observations. J. Neurol. Sci. 81, 301–320. https://doi.org/10.1016/0022-510X(87)90105-5.
Ono, S., Inoue, K., Mannen, T., Mitake, S., Shirai, T., Kanda, F., Jinnai, K., Takahashi, K., 1989. Intracytoplasmic inclusion bodies of the thalamus and the substantia nigra, and Marinesco bodies in myotonic dystrophy: a quantitative morphological study. Acta Neuropathol. 77, 350–356. https://doi.org/10.1007/BF00687369.
Popescu, B.F.G., Lucchinetti, C.F., 2012. Pathology of demyelinating diseases. Annu. Rev. Pathol. 7, 185–217. https://doi.org/10.1146/annurev-pathol-011811-132443.
Raz, E., Cercignani, M., Sbardella, E., Totaro, P., Pozzilli, C., Bozzali, M., Pantano, P., 2010. Clinically isolated syndrome suggestive of multiple sclerosis: voxelwise regional investigation of white and gray matter. Radiology 254, 227–234. https://doi.org/10.1148/radiol.2541090817. Epub 2009 Dec 17.
Romeo, V., 2012. Myotonic dystrophy type 1 or Steinert's disease. Adv. Exp. Med. Biol. 724, 239–257.
Schara, U., Schoser, B.G.H., 2014. Myotonic dystrophies type 1 and 2: a summary on current aspects. Semin. Pediatr. Neurol. 13, 71–79. https://doi.org/10.1016/j.spen.2006.06.002.
Schmierer, K., Tozer, D.J., Scaravilli, F., Altmann, D.R., Barker, G.J., Tofts, P.S., Miller, D.H., 2007. Quantitative magnetization transfer imaging in postmortem multiple sclerosis brain. J. Magn. Reson. Imaging 26, 41–51. https://doi.org/10.1002/jmri.20984.
Serra, L., Cercignani, M., Bruschini, M., Cipolotti, L., Mancini, M., Silvestri, G., Petrucci, A., Bucci, E., Antonini, G., Licchelli, L., Spanò, B., Giacanelli, M., Caltagirone, C., Meola, G., Bozzali, M., Artero, R., 2016. "I Know that You Know that I Know": neural substrates associated with social cognition deficits in DM1 patients. PLoS One 11 (6), e0156901. https://doi.org/10.1371/journal.pone.0156901.
Serra, L., Silvestri, G., Petrucci, A., Basile, B., Masciullo, M., Makovac, E., Torso, M., Spanò, B., Mastropasqua, C., Harrison, N.A., Bianchi, M.L.E., Giacanelli, M., Caltagirone, C., Cercignani, M., Bozzali, M., 2014. Abnormal functional brain connectivity and personality traits in myotonic dystrophy type 1. JAMA Neurol. 71, 603–611. https://doi.org/10.1001/jamaneurol.2014.130.
Serra, L., Petrucci, A., Spanò, B., Torso, M., Olivito, G., Lispi, L., Costanzi-Porrini, S., Giulietti, G., Koch, G., Giacanelli, M., Caltagirone, C., Cercignani, M., Bozzali, M., 2015. How genetics affects the brain to produce higher level dysfuctions in myotonic dystrophy type 1. Funct. Neurol. 30, 21–31.
Serra, L., Bianchi, G., Bruschini, M., Giulietti, G., Domenico, C.D., Bonarota, S., Petrucci, A., Silvestri, G., Perna, A., Meola, G., Caltagirone, C., Bozzali, M., 2020. Abnormal cortical thickness is associated with deficits in social cognition in patients with myotonic dystrophy type 1. Front. Neurol. 11, 113. https://doi.org/10.3389/fneur.2020.00113.
Sled, J.G., 2018. Modelling and interpretation of magnetization transfer imaging in the brain. Neuroimage 182, 128–135. https://doi.org/10.1016/j.neuroimage.2017.11.065.
Spanò, B., Giulietti, G., Pisani, V., Morreale, M., Tuzzi, E., Nocentini, U., Francia, A., Caltagirone, C., Bozzali, M., Cercignani, M., 2018. Disruption of neurite morphology parallels MS progression. Neurol. Neuroimmunol. Neuroinflamm. 5, e502. https://doi.org/10.1212/NXI.0000000000000502.
Stanisz, G.J., Webb, S., Munro, C.A., Pun, T., Midha, R., 2004. MR properties of excised neural tissue following experimentally induced inflammation. Magn. Reson. Med. 51, 473–479. https://doi.org/10.1002/mrm.20008. PMID: 15004787.
Tallantyre, E.C., Brookes, M.J., Dixon, J.E., Morgan, P.S., Evangelou, N., Morris, P.G., 2008. Demonstrating the perivascular distribution of MS lesions in vivo with 7-Tesla MRI. Neurology 70, 2076–2078. https://doi.org/10.1212/01.wnl.0000313377.49555.2e.
Thornton, C.A., Johnson, K., Moxley, R.T., 1994. Myotonic dystrophy patients have larger CTG expansions in skeletal muscle than in leukocytes. Ann. Neurol. 35, 104–107. https://doi.org/10.1002/(ISSN)1531-824910.1002/ana.v35:110.1002/ana.410350116.
Turati, L., Moscatelli, M., Mastropietro, A., Dowell, N.G., Zucca, I., Erbetta, A., Cordiglieri, C., Brenna, G., Bianchi, B., Mantegazza, R., Cercignani, M., Baggi, F., Minati, L., 2015. In vivo quantitative magnetization transfer imaging correlates with histology during de- and remyelination in cuprizone-treated mice. NMR Biomed. 28, 327–337. https://doi.org/10.1002/nbm.3253.
Turner, C., Hilton-Jones, D., 2014. The myotonic dystrophies: diagnosis and management. Curr. Opin. Neurol. 27, 599–606. https://doi.org/10.1097/WCO.0000000000000128.
van der Plas, E., Hamilton, M.J., Miller, J.N., Koscik, T.R., Long, J.D., Cumming, S., Povilaikaite, J., Farrugia, M.E., McLean, J., Jampana, R., Magnotta, V.A., Gutmann, L., Monckton, D.G., Nopoulos, P.C., 2019. Brain structural features of myotonic dystrophy type 1 and their relationship with CTG repeats. J. Neuromuscul. Dis. 6, 321–332. https://doi.org/10.3233/JND-190397.
Vermersch, P., Sergeant, N., Ruchoux, M.M., Hofmann-Radvanyi, H., Wattez, A., Petit, H., Dewailly, P., Delacourte, A., 1996. Specific tau variants in the brains of patients with myotonic dystrophy. Neurology 47, 711–717. https://doi.org/10.1212/WNL.47.3.711.
Vielhaber, S., Jakubiczka, S., Gaul, C., Schoenfeld, M.A., Debska-Vielhaber, G., Zierz, S., Heinze, H.-J., Niessen, H.G., Kaufmann, Jörn, 2006. Brain 1H magnetic resonance spectroscopic differences in myotonic dystrophy type 2 and type 1. Muscle Nerve 34, 145–152. https://doi.org/10.1002/(ISSN)1097-459810.1002/mus.v34:210.1002/mus.20565.
Weber, Y.G., Roebling, R., Kassubek, J., Hoffmann, S., Rosenbohm, A., Wolf, M., Steinbach, P., Jurkat-Rott, K., Walter, H., Reske, S.N., Lehmann-Horn, F., Mottaghy, F.M., Lerche, H., 2010. Comparative analysis of brain structure, metabolism, and cognition in myotonic dystrophy 1 and 2. Neurology 74, 1108–1117. https://doi.org/10.1212/WNL.0b013e3181d8c35f.
Wolff, S.D., Balaban, R.S., 1989. Magnetization transfer contrast (MTC) and tissue water proton relaxation in vivo. Magn. Reson. Med. 10, 135–144. https://doi.org/10.1002/mrm.1910100113.
Yoshimura, N., Otake, M., Igarashi, K., Matsunaga, M., Takebe, K., Kudo, H., 1990. Topography of Alzheimer's neurofibrillary change distribution in myotonic dystrophy. Clin. Neuropathol. 9, 234–239.
Zanigni, S., Evangelisti, S., Giannoccaro, M.P., Oppi, F., Poda, R., Giorgio, A., Testa, C., Manners, D.N., Avoni, P., Gramegna, L.L., De Stefano, N., Lodi, R., Tonon, C., Liguori, R., 2016. Relationship of white and gray matter abnormalities to clinical and genetic features in myotonic dystrophy type 1. Neuroimage Clin. 11, 678–685. https://doi.org/10.1016/j.nicl.2016.04.012.